Robust adiabatic sum frequency conversion

Haim Suchowski[1], Vaibhav Prabhudesai[1], Dan Oron[1], Ady Arie[2] and Yaron Silberberg[1]

[1]*Physics of Complex System, Weizmann Institute of Science, Rehovot, 76100, Israel*
[2]*School of Electrical Engineeing, Faculty of Engineering, Tel Aviv University, Ramat Aviv, 69978, Israel*

Abstract: We discuss theoretically and demonstrate experimentally the robustness of the adiabatic sum frequency conversion method. This technique, borrowed from an analogous scheme of robust population transfer in atomic physics and nuclear magnetic resonance, enables the achievement of nearly full frequency conversion in a sum frequency generation process for a bandwidth up to two orders of magnitude wider than in conventional conversion schemes. We show that this scheme is robust to variations in the parameters of both the nonlinear crystal and of the incoming light. These include the crystal temperature, the frequency of the incoming field, the pump intensity, the crystal length and the angle of incidence. Also, we show that this extremely broad bandwidth can be tuned to higher or lower central wavelengths by changing either the pump frequency or the crystal temperature. The detailed study of the properties of this converter is done using the Landau-Zener theory dealing with the adiabatic transitions in two level systems.

OCIS codes: (190.4360) Nonlinear optics; (140.3613) Laser and laser optics; (230.4320) Optical devices.

References and links

1. F. Bloch, "Nuclear Induction", Phys. Rev. **70**, 460-474 (1946).
2. R. P. Feynman, F. L. Vernon, and R. W. Hellwarth, "Geometrical Representation of the Schrodinger Equation for Solving Maser Problems", J. Appl. Phys. **28**, 49-52 (1957).
3. H. Suchowski, D. Oron, A. Arie, and Y. Silberberg, "Geometrical Representation of Sum Frequency Generation and Adiabatic Frequency Conversion", Phys. Rev. A, **78**, 063821 (2008).
4. D. Boyd, *Nonlinear Optics*, 2nd ed. (Academic, New York, 2003).
5. A. Yariv, *Quantum Electronics*, 3rd ed. (Wiley, 1989).
6. L. Allen and J. H. Eberly, *Optical Resonance and Two Level Atoms* (Dover, New York, 1987).
7. T. Torosov and N. V. Vitanov, "Exactly soluble two-state quantum models with linear couplings", J. Phys. A, **41**, 155309 (2008).
8. G. Imeshev, M. Fejer, A. Galvanauskas, and D. Harter, "Pulse shaping by difference-frequency mixing with quasi-phase-matching gratings", J. Opt. Soc. Am. B **18**, 534-539 (2001).
9. M. Arbore, A. Galvanauskas, D. Harter, M. Chou, and M. Fejer, "Engineerable compression of ultrashort pulses by use of second-harmonic generation in chirped-period-poled lithium niobate" Opt. Lett. **22**, 1341-1343 (1997).
10. G. Imeshev, M. Arbore, M. Fejer, A. Galvanauskas, M. Fermann, and D. Harter, "Ultrashort-pulse second-harmonic generation with longitudinally nonuniform quasi-phase-matching gratings: pulse compression and shaping", J. Opt. Soc. Am. B, **17**, 304-318 (2000).
11. D. S. Hum, and M. Fejer, "Quasi-phasematching", C. R. Physique **8**, 180-198 (2007).
12. M. Charbonneau-Lefort, B. Afeyan, and M. Fejer, "Optical parametric amplifiers using chirped quasi-phasematching gratings. I. Practical design formulas", J. Opt. Soc. Am. B **25**, 463-480 (2008).
13. M. Baudrier-Raybaut, R. Haidar, Ph. Kupecek, Ph. Lemasson, and E. Rosencher, "Random quasi phase matching in bulk polycrystalline isotropic nonlinear materials", Nature **432**, 374-376 (2004).

#108558 - $15.00 USD Received 11 Mar 2009; revised 14 May 2009; accepted 26 May 2009; published 13 Jul 2009

14. K. Mizuuchi, K. Yamamoto, M. Kato, and H. Sato, "Broadening of the Phase-Matching Bandwidth in Quasi-Phased-Matched Second Harmonic Generation", IEEE J. Quantum Electron **30**, 15961604 (1994).
15. L. D. Landau, "Zur Theorie der Energieubertragung. II", Physics of the Soviet Union **2**, 46-51 (1932).
16. C. Zener, "Non-adiabatic Crossing of Energy Levels", Proc. Roy. Soc. London A **137**, 696-702 (1932).
17. A. Massiach, *Quantum Mechanics* (N. Holland, Amsterdam, 1962), Vol II.
18. D. J. Tannor, *Introduction to Quantum Mechanics: A Time-dependent Perspective* (University Science Books, Sausalito, California, 2007).
19. J. Armstrong, N. Bloembergen, J. Ducuing, and P. Pershan, "Interactions between Light Waves in a Nonlinear Dielectric", Phys. Rev. **127**, 1918-1939 (1962).
20. G. Rosenman, A. Skliar and D.Eger, M. Oron, and M. Katz, "Low temperature periodic electrical poling of flux-grown $KTiOPO_4$ and isomorphic crystals", Appl. Phys. Lett., **73**, 3650-3652 (1998).
21. S. Emanueli, and A. Arie, "Temperature-Dependent Dispersion Equations for $KTiOPO_4$ and $KTiOAsO_4$", Appl. Opt. **42**, 6661-6665 (2003).

1. Introduction

Nonlinear frequency conversion via three wave mixing process is a fundamental concept in the field of nonlinear optics. In this process, light of two colors is mixed in a nonlinear crystal, resulting in the generation of a third color with their sum or difference frequency. These processes (also termed frequency up-conversion and down-conversion, respectively) usually exhibit a tradeoff between the conversion bandwidth and the conversion efficiency.

Recently, we have shown that the sum frequency generation (SFG) process in the undepleted pump approximation can be mathematically formulated and geometrically visualized in complete analogy with the framework of a two-level system, as introduced by Bloch in NMR and Feynman and coworkers in atomic physics [1, 2]. In this regime the conversion process is governed by a set of two linear coupled wave equations whose properties depend on two parameters: the phase mismatch along the propagation direction and the coupling coefficient, which is a function of both the characteristics of the pump wave and the properties of the nonlinear crystal. The geometrical visualization gives physical intuition to the process of SFG [3].

In the usual scheme of sum frequency generation, these two parameters are assumed to be constant, and thus the evolution of these waves along the propagation axis can be solved analytically [4, 5, 6]. Only few more analytic solutions of this form of linear coupled wave equations, which exhibit SU(2) dynamical symmetry, are known. Those were recently summarized in the context of atomic physics by Torosov *et. al.* [7], where most of them have not been implemented in the field of frequency conversion. Two approximate solutions to this set of equations are worth mentioning in this context. The first is the perturbative approximation, which in the realm of frequency conversion is the case of weak coupling between the signal and idler waves. This approximation was termed as the 'unamplified signal approximation', and corresponds to a low signal-to-idler conversion efficiency. With the perturbative approximation, the dynamics of the process can be fully solved either in real space or using Fourier domain as done by Imeshev *et. al.* [8]. The second approximation is the adiabatic approximation. By exploring the application of the rapid adiabatic passage (RAP) scheme [6] in the realm of frequency conversion, we have shown that the requirements of high efficiency and broad bandwidth can be reconciled, by adiabatically varying the phase mismatch parameter along the propagation, allowing nearly complete transfer of energy from one wavelength to another in a robust manner [3]. The detailed study of the properties of this converter is done using the Landau-Zener theory dealing with adiabatic transitions in two level systems [15, 16].

The implementation of this converter is done by aperiodically poling in a quasi-phased matched crystal. Such structures were extensively studied in the last decade, mainly due to the fact that they enable the tailoring of desired phase mismatching function in a simple manner. Linear chirp gratings were shown to have broad response also in second harmonic generation (SHG), difference frequency generation (DFG) and optical parametric amplifier (OPA) and

#108558 - $15.00 USD Received 11 Mar 2009; revised 14 May 2009; accepted 26 May 2009; published 13 Jul 2009

other nonlinear processes [9, 10, 11, 12]. Random structures [13] and segmented structures [14] were also suggested to improve bandwidth response in nonlinear processes, but again with poor efficiency. It should be noted that the dynamics of different nonlinear processes are affected differently by these aperiodic structures. *Only* in SFG process, the geometrical visualization on Bloch sphere, and the suggested adiabatic solution are valid.

In this paper, we demonstrate the robustness of the adiabatic SFG scheme to most of the parameters which control the efficiency of the process. These include the crystal temperature, the frequency of the incoming field, the pump intensity, the crystal length and the angle of incidence. We show that contrary to the conventional perfect phase-matched crystal, where simultaneous matching of these control parameters are needed, in this scheme, the conversion efficiency is insensitive to change of one or more of those parameters. Also, we demonstrate that this ultra broad bandwidth converter can be tuned to higher or lower central wavelengths by changing either the pump frequency or the crystal temperature.

2. Theoretical analysis

2.1. Dynamics and Geometrical Representation of Sum Frequency Generation Process

In the undepleted pump approximation, the pump amplitude is assumed constant along the nonlinear crystal, and the following normalized coupled equations for the signal and idler can be constructed [4]:

$$\frac{d\tilde{A}_1}{dz}+\frac{1}{v_{g_1}}\frac{d\tilde{A}_1}{dt} = -i\kappa\tilde{A}_3e^{-i\Delta kz} \quad (1)$$

$$\frac{d\tilde{A}_3}{dz}+\frac{1}{v_{g_3}}\frac{d\tilde{A}_3}{dt} = -i\kappa^*\tilde{A}_1e^{+i\Delta kz} \quad (2)$$

where $\Delta k = k_1 + k_2 - k_3$ is the phase mismatch, z is the position along the propagation axis, $\kappa = \frac{4\pi\omega_1\omega_3}{\sqrt{k_1k_3}c^2}\chi^{(2)}A_2$ is the coupling coefficient. The normalized signal and idler amplitudes are: $\tilde{A}_1 = \frac{c}{4\omega_1}\sqrt{\frac{k_1}{\pi\chi^{(2)}A_2^*}}A_1$ and $\tilde{A}_3 = \frac{c}{4\omega_3}\sqrt{\frac{k_3}{\pi\chi^{(2)}A_2}}A_3$, where ω_1 and ω_3 are the frequencies of the signal and idler, respectively, k_1 and k_3 are their wave numbers, v_{g_1} and v_{g_3} are their group velocities, c is the speed of light in vacuum, A_1, A_2, A_3 are the signal, pump and idler amplitudes, respectively, and $\chi^{(2)}$ is the 2^{nd} order susceptibility of the crystal (assumed to be frequency independent). In the case where the temporal envelope of the waves are much longer than the length of the crystal (i.e. where we consider monochromatic, quasi-monochromatic laser beams, or stretched ultrashort pulses), one can omit the influence of the waves' group velocities. In this paper we will deal with quasi-monochromatic laser beams. In the case of ultrashort pulses upconversion, one should first stretch the pulse, in order to minimize the deleterious effect of group velocity mismatch and group velocity dispersion. Typically, a pulse length of more than 1ps would suffice for an interaction in the visible and near infrared. The converted pulse would be re-compressed to a transform-limited pulse after exiting from the nonlinear crystal.

As discussed earlier, these coupled wave equations, have the same form as those describing the dynamics of quantum mechanical two level systems. Here, the time evolution is replaced by propagation in the longitudinal z-axis, and the detuning Δ is replaced by the phase-mismatch Δk value; also, the population of the ground and excited states are analogous to the magnitude of the signal and idler fields, respectively. This analogy is further detailed in Ref. [3]. To obtain a physical intuition of the SFG dynamics, we use the geometrical picture of this process, where we adopt the formulation of Feynman *et. al.* [2]. In this framework, a real three dimensional vector equation can explore the dynamics of this problem, and any z-dependent

#108558 - $15.00 USD Received 11 Mar 2009; revised 14 May 2009; accepted 26 May 2009; published 13 Jul 2009

function of $\Delta k(z)$ and $\kappa(z)$, can be visualized as a trajectory on the surface of an upconversion Bloch sphere. The loss-free evolution equations can be written as a single vector precession equation $\frac{d\vec{\rho}_{SFG}}{dz} = \vec{g} \times \vec{\rho}_{SFG}$, where the three dimensional state vector is defined as follows $\vec{\rho}_{SFG} = (U,V,W) = \left(A_3^* A_1 + A_3 A_1^*, i(A_3^* A_1 - A_3 A_1^*), |A_3|^2 - |A_1|^2\right)$, and includes the coherence between the signal and idler amplitudes along the propagation. In particular, its z component (W_{SFG}) gives information about the conversion efficiency. The south pole $\vec{\rho} = (0,0,-1)$ corresponds to zero conversion ($A_3 = 0$), while the north pole $\vec{\rho} = (0,0,1)$ corresponds to full conversion. In between, the conversion efficiency is defined as: $\eta = (W_{SFG} + 1)/2$. The rotating vector (also known as the torque vector), $\vec{g} = (Re\{\kappa\}, Im\{\kappa\}, \Delta k)$, represents the coupling between the signal and idler frequencies, and the size of the phase mismatch parameter. This analogy was extended to include the semi-phenomenological decay constants T_1 and T_2, which appear in the original Bloch equations, and in our context are characteristic decay lengths rather than times [3]. As seen, the evolution of the SFG process is dictated by $\Delta k(z)$ and κ, and in most of the cases, no analytical or approximate solution exists. In such cases, the geometrical visualization could be helpful, where the trajectory of the SFG process, for any function of $\Delta k(z)$ and $\kappa(z)$, is guaranteed to be on the surface of the SFG Bloch sphere.

2.2. Adiabaticity criteria and application of Landau-Zener theory

One important approximation to this dynamical problem is the adiabatic solution. In this case, the first derivative of the phase mismatch parameter along the propagation axis, also known as the sweep rate, should vary slowly with respect to the square of the coupling term, i.e.

$$\left|\frac{d\Delta k}{dz}\right| << \frac{\left(\Delta k^2 + \kappa^2\right)^{3/2}}{\kappa}. \tag{3}$$

For an efficient and broadband process to occur, the phase mismatch parameter, $\Delta k(z)$ should also be very large compared to κ, and should change adiabatically from a large negative value to a large positive value, i.e. $|\Delta k| >> \kappa$, $\Delta k(z=0) < 0$, $\Delta k(z=L) > 0$. These adiabatic constraints were derived by following their analogous dynamical counterparts in the RAP mechanism, where a strong chirped excitation pulse scans slowly through the resonance to achieve robust full inversion [7, 17, 18]. If the rate of variation is not slow enough, or the coupling coefficient is not large enough, this inequality will not be satisfied and the conversion efficiency will be poor. Clearly, in any practical realization, where the crystal length is finite, the adiabaticity condition, corresponding to a conversion efficiency of 100%, can only be asymptotically reached. Note again, that all of the adiabatic constraints have to be satisfied in order to achieve this robust mechanism. This explains why in the case of constant phase mismatch (such as in periodically poled crystal), where the sweep rate is zero, and although the requirement of Eq. 3 is satisfied, adiabatic conversion would not occur.

When the phase-mismatched $\Delta k(z)$ is varied linearly along the crystal, a simple parameter for the degree of adiabaticity appears. In the quantum literature it is known as the Landau-Zener criterion [15, 16], which in the frequency conversion realm can be written as:

$$\eta_{LZ}(z \to \infty) = 1 - e^{-\frac{4\kappa^2}{\pi |d\Delta k/dz|}}. \tag{4}$$

This analytical expression gives the signal-to-idler conversion efficiency of the SFG process at the output of the nonlinear crystal. It depends exponentially on an adiabatic parameter, defined as $\alpha \equiv \frac{\pi |d\Delta k/dz|}{4\kappa^2}$, i.e. the ratio between the sweep rate of the phase mismatch, $d\Delta k/dz$, and the square of the coupling coefficient, κ^2. Mathematically this represents the ratio between the left hand side and the right hand side of Eq. 3, at the location where $\Delta k = 0$. *Adiabatic* propagation

#108558 - $15.00 USD Received 11 Mar 2009; revised 14 May 2009; accepted 26 May 2009; published 13 Jul 2009

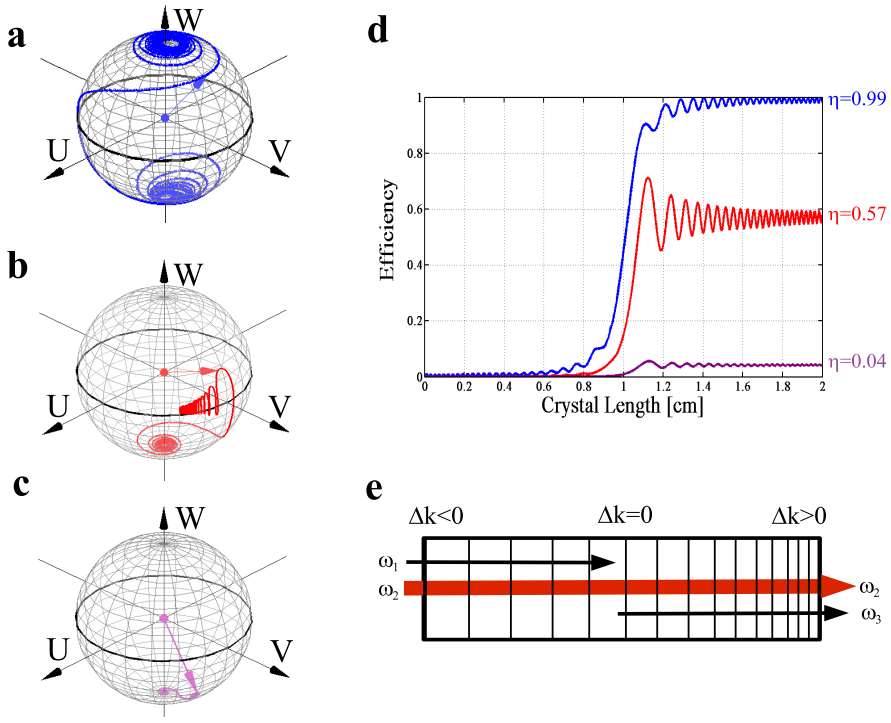

Fig. 1. Bloch sphere trajectories of SFG of three different intensities (a) (Media 1) $440MW/cm^2$ (b) (Media 2) $80MW/cm^2$ (c) (Media 3) $4MW/cm^2$. The south-pole represents the amplitude of the input frequency, and the north-pole represents the amplitude of the converted frequency. (d) The projection of the trajectories onto the W axis yields the conversion efficiency along the propagation. In these trajectories, phase matching condition is fulfilled at z=1cm. The predicted output conversion efficiency for each trajectory, based on Eq. 4, is also presented. (e) Continuous adiabatic variation of the phase mismatch parameter is required. This can be achieved by slowly changing the poling periodicity along the propagation direction.

is obtained when $\alpha << 1$, which is the case where the conversion efficiency reaches unity. This can be achieved either by changing slowly the sweep rate at a given pump intensity, or by applying strong pump for a given sweep rate.

In Fig. 1 we present three cases of the SFG dynamics when a linear sweep rate is applied. When $\alpha << 1$, full frequency conversion is achieved as shown in Fig. 1(a). When, the pump intensity is not high enough or the sweep rate at a given crystal length and pump intensity is not slow enough, then $\alpha \sim 1$, and the conversion efficiency will drop, as seen in Fig. 1(b). The case of $\alpha >> 1$, is where the pump intensity is small, or the sweep rate is extremely high. This corresponds to the weak coupling regime (the "unamplified signal approximation"), which results in low conversion efficiency, as shown in Fig. 1(c). These dynamical trajectories can be projected on the W-axis of the sphere, bringing information regarding the conversion efficiency along the propagation, as shown in Fig. 1(d). Also, their calculated Landau-Zener conversion efficiencies are presented to the right of each projected trajectory. Due to the importance of Eq.

#108558 - $15.00 USD Received 11 Mar 2009; revised 14 May 2009; accepted 26 May 2009; published 13 Jul 2009

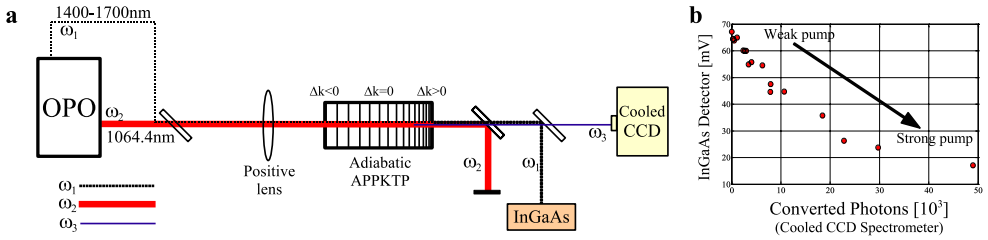

Fig. 2. (a) The adiabatic sum frequency conversion apparatus. The detection stage was designed to detect both the incoming ω_1 beam, with the InGaAs detector, and the converted ω_3 beam, with the cooled CCD detection. (b) The monotonic relation between the growth of the converted beam (measured by a cooled CCD spectrometer) with the decrease of the incoming beam (measured by an InGaAs detector), when increasing the pump intensity.

4, we decided to present it in more practical parameters:

$$\eta_{LZ}(z\to\infty)=1-exp\left(-\frac{2^5\cdot 3^2\cdot 10^{-3}\pi^2\left(\chi^{(2)}\right)^2 I_2}{n_1n_2n_3\lambda_1\lambda_3 c|d\Delta k/dz|}\right). \tag{5}$$

Here, $c=3\cdot 10^{10}\,cm/sec$, λ_1 and λ_3 are measured in cm, I_2 is measured in MW/cm^2, $\chi^{(2)}$ is measured in pm/V and $|d\Delta k/dz|$ is measured in cm^{-2}.

3. Experimental setup and results

Although other implementations are possible, the simplicity and robustness of the quasi-phase matching technique [19] in manipulating of the phase mismatch parameter, makes it the most attractive in terms of experimental realization. The desired value of the phase-mismatch parameter is obtained by tuning the spatial structure of the domains using the approximate relation: $\Delta k_\Lambda(z)=\frac{2\pi}{\Lambda(z)}$, where $\Lambda(z)$ is the local poling period.

By proper design of the periodicity of the poling, satisfying the adiabatic constraints posed by Eq. 3, an effective phase mismatch function was obtained,

$$\Delta k_{eff}(z)=k_1(z)+k_2(z)-k_3(z)+\Delta k_\Lambda(z)=\Delta k_{proc}(z)+\Delta k_\Lambda(z). \tag{6}$$

Generally, for an aperiodic design it is reasonable to expand $\Delta k_\Lambda(z)$ in a power series: $\Delta k_\Lambda(z)=\Delta k_0+\frac{\partial\Delta k}{\partial z}z+\frac{1}{2}\frac{\partial^2\Delta k}{\partial z^2}z^2+...\frac{1}{N!}\frac{\partial^N\Delta k}{\partial z^N}z^N$. For simplicity we chose to design the adiabatic aperiodically poled structure, with only two non-zero terms: the constant term, choosing $\Delta k_0=-\Delta k_{proc}(z=L/2)$, and the linear term, $\frac{\partial\Delta k}{\partial z}$, chose to satisfy the adiabatic constraint posed by inequality 3. It is important to note that this simple design is not generally optimal in the sense of SFG bandwidth or temperature response. A more accurate solution for $\Delta k_\Lambda(z)$, should take into account the spectral dependence of $\Delta k_{proc}(z)$, due to dispersion, as well as the spectral variation of the coupling constant. In practice, in the near-mid IR regime, these higher order corrections are relatively small.

The particular design used in the experiments was tested by numerical simulations of the propagation process using the finite difference method, where the periodicity was varied from 14.6 μm to 16.2 μm along a flux-grown $KTiOPO_4$ crystal (Raicol Crystals Ltd.), with dimensions of 20 x 2 x 1 mm. It was poled by low-temperature electric-field poling [20]. A plane wave approximation, and a nonlinear susceptibility $\chi^{(2)}=32\frac{pm}{V}$ were assumed. The experimental apparatus is shown in Fig. 2(a). We used an optical parametric oscillator (Ekspla NT342) as our

#108558 - $15.00 USD Received 11 Mar 2009; revised 14 May 2009; accepted 26 May 2009; published 13 Jul 2009

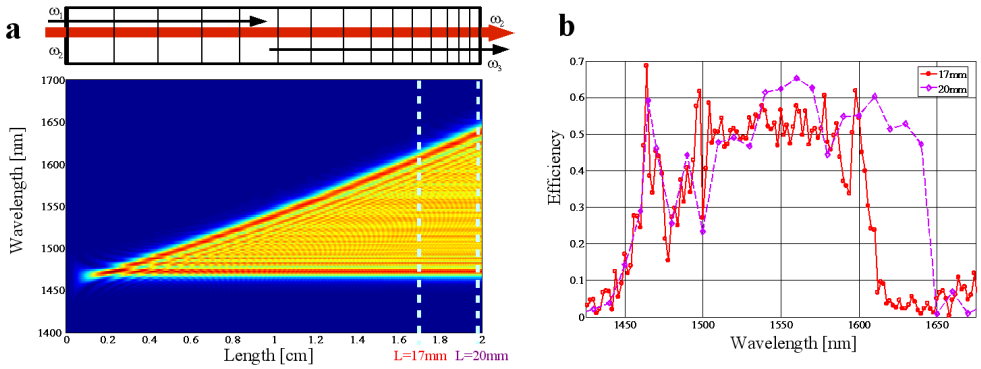

Fig. 3. Conversion efficiency as a function of input wavelength and the crystal length. (a) Two dimensional numerical simulation of the conversion efficiency as a function of input wavelength (y axis), and propagation distance. As seen, the shorter wavelengths are being converted early along the crystal, and the longer wavelengths are being converted as the crystal length is increased. (b) Experimental results of the spectral response in two different crystal length, 17 mm and 20 mm.

laser sources for both a strong pump at 1064 nm (6 ns, 130 μJ), and a tunable signal varied from 1400 nm to 1700 nm (5 ns, 1μJ). The pump and the signal, both polarized in the extraordinary axis were spatially overlapped and focused collinearly into the crystal having waists of 150μm and 120μm, respectively. These values guarantee that the Rayleigh range is larger than the crystal length and thus the plane wave approximation of our simulations holds. The crystal was held in a temperature-controlled mount. We collected both the input wavelength (signal) and output SFG wavelength (idler) after their propagation in the crystal and recorded them using an InGaAs photodiode, and a cooled CCD spectrometer, respectively.

Our demonstration consists of several sets of experiments. In each set, we varied a different parameter of the process. Two of these sets were discussed briefly in Ref. [3], and here those are mentioned for completeness. In all the experiments, the conversion efficiency was measured by comparing the signal intensity with and without the presence of the pump beam. This was done after verifying that the increase of the converted beam, A_3, is correlated with the power loss of the incoming beam, A_1, as shown in Fig 2(b).

First, we measured the conversion efficiency as a function of the pump peak intensity for a fixed signal wavelength 1530 nm. The results are presented in Fig. 2(b). A very good correspondence was obtained with the numerical simulation, where the maximal efficiency which was achieved with our maximal pump intensity was $74\% \pm 3\%$ [3]. It is important to note that unlike the case of a phase-matched crystal, where the conversion efficiency oscillates between unity and zero upon increase in the pump intensity, the conversion efficiency would remain nearly unity also for pump intensities exceeding $360 MW/cm^2$.

In the second set of experiments, we measured the conversion efficiency as a function of the input wavelength, at a moderate pump intensity of 60 MW/cm^2. It was shown that an efficient ultra-broadband conversion of over 140nm wide (1470nm to 1610nm) at room temperature was obtained, except for a small region of low efficiency around 1485nm, which was associated with a local fabrication defect, leading to violation of the adiabaticity condition at this wavelength [3]. By performing these measurements for two different lengths, 17mm and 20mm, of the same crystal, the robustness of our design to variations in the crystal length is also demon-

#108558 - $15.00 USD Received 11 Mar 2009; revised 14 May 2009; accepted 26 May 2009; published 13 Jul 2009

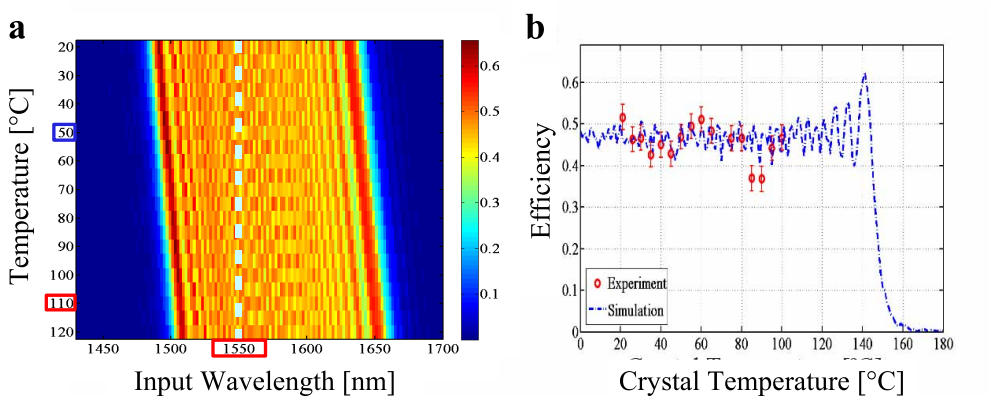

Fig. 4. Conversion efficiency as a function of crystal temperature, using the adiabatic aperiodically poled KTP design at a pump intensity of $60MW/cm^2$. (a) Two dimensional numerical simulation of the conversion efficiency as a function of crystal temperature (y-axis) and input wavelength. (b) Conversion efficiency as a function of crystal temperature at constant input wavelength of $\omega_1 = 1550nm$. A good correspondence between the experimental results and the simulation of the design (vertical cross section of the two dimensional simulation) is shown.

strated. In contrast to frequency converter, where the use of thin crystals is required to achieve maximal bandwidth, in the adiabatic design the achieved bandwidth is expected to grow as the crystal length increases, while maintaining the same conversion efficiency. We show this both numerically and experimentally in Fig. 3. As can be seen, the efficient conversion bandwidth is increased almost linearly with the length of the crystals. This is in good agreement with the experimental results of Fig. 3(b), which show a 30nm wider bandwidth response as the increasing of the crystal length in 3 mm. Two factors practically limit the achievable efficient conversion bandwidth. The first is absorption in the nonlinear crystal itself. Another limiting factor arises from the plane wave approximation which holds only if the crystal length is shorter than the apparatus Rayleigh range. The latter is, in practice, limited by the available pump energy.

This broad response can also be maintained by varying the temperature of the nonlinear crystal. This affects the conversion process both due to the temperature dependence of the crystal's refractive index, as well as through thermal expansion of the aperiodically poled structure. This secondary, but crucial effect, causes the expansion of the domains while increasing the temperature, effectively decreasing the phase mismatch parameter along the propagation. This leads to a weaker temperature response than that determined by the adiabatic design. In standard frequency conversion, temperature has a dramatic effect on the conversion efficiency and in fact, temperature tuning is commonly used to spectrally tune the narrow conversion bandwidth. In contrast, for the adiabatic design, the conversion efficiency remains high even for large variation in the crystal temperature. In Fig. 4(a) we present a numerical simulation of the conversion efficiency as a function of the input wavelength and the temperature of the crystal. In this plot, every vertical cross section represents the conversion efficiency as a function of crystal temperature for a constant wavelength. The experimental results are shown in Fig. 4(b), were the conversion efficiency at a constant wavelength of $\omega_1 = 1550nm$ as function of the crystal temperature is plotted. Highly efficient conversion is experimentally observed in a temperature range of over 80^oC. The simulation, which contains the effect of thermal expansion (taken from Ref. [21]), predicts that this range exceeds, in fact, beyond the limit of our experiment. This is

#108558 - $15.00 USD Received 11 Mar 2009; revised 14 May 2009; accepted 26 May 2009; published 13 Jul 2009

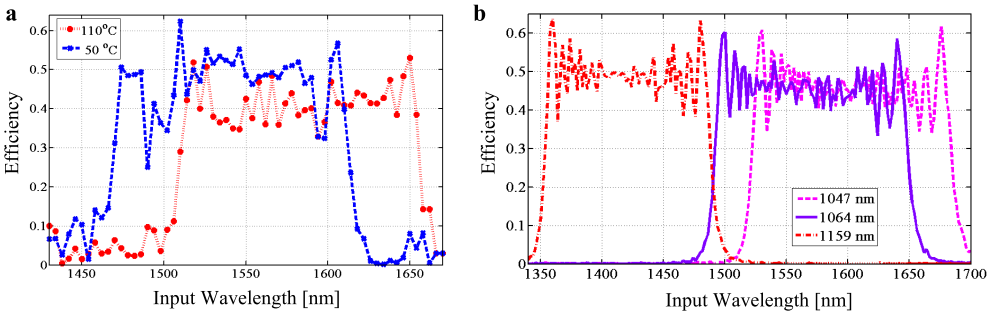

Fig. 5. Tunability of the broad bandwidth response. (a) Experimental results of temperature tunability, at pump intensity of $60MW/cm^2$ Conversion efficiency. This shows a good agreement with the numerical simulations, presented in figure 4. (b) Numerical simulations of pump wavelength tunability.

to be compared with an efficient range of 2^oC in the case of SFG in a phase matched crystal, obtained by periodic poling.

Another important parameter, which usually influences the phase mismatch is the incident angle of the incoming frequencies with the nonlinear crystal. We checked, in simulations only, the robustness of the adiabatic design, and found out that the acceptance angle of our design had increased from less than 5 degrees in the periodically poled structure to more than 25 degrees, for input wavelength of $\omega_1 = 1550nm$, and crystal length of $L = 20mm$.

Last, we would like to show that the adiabatic design is not only broad and robust, but that it can, for a given crystal design, also be tuned in a broad range. This is done by two separate mechanisms: temperature tuning and pump frequency tuning, enabling us to shift the efficient conversion band to lower or higher input frequencies. In Fig. 5(a), we plot the measured conversion efficiency as a function of input wavelength for two crystal temperatures: 50^oC and 110^oC. As can be seen, the efficient conversion band is redshifted by $\approx 50nm$, which is in good correspondence with the numerical simulations shown,as horizontal cross sections, in Fig. 4(a). The horizontal 1D cross-sections of the 2D numerical simulation would give the expected bandwidth in each crystal temperature. The two experimental values are marked at the left of the figure, and use the same color definition (blue for 50^oC and red for 110^oC). An even more dramatic effect is presented in Fig. 5(b), where the effect of changing the pump wavelength is simulated. In the figure we compare the response of our adiabatic design pumped at 1064nm (as in the experiments) with the response to a pump wavelength of 1047 nm (pumping with a Nd:YLF laser), and pump wavelength of 1159 nm, which can be readily obtained by raman shifting the 1064nm excitation beam, in a Raman shifter.
In both tuning mechanisms, we see that as the efficient conversion band is tuned to lower wavelengths, the conversion efficiency slightly increases and the response becomes slightly narrower. Tuning to the higher wavelength leads to the opposite behavior. The change in conversion efficiency is a direct outcome from the fact that the coupling coefficient was changed (decreased or increased, respectively), mainly through its dependence on the characteristics of the pump. This effectively changes the adiabatic parameter, and thus the conversion efficiency. The narrowing or broadening of the spectral response merely reflects the constant bandwidth in frequency.

4. Conclusion

In this paper we analyzed the robustness of the adiabatic sum frequency generation scheme. We showed that it exhibits efficient conversion for wide range of frequencies and temperatures, up

#108558 - $15.00 USD Received 11 Mar 2009; revised 14 May 2009; accepted 26 May 2009; published 13 Jul 2009

to two orders of magnitude larger than a standard phase matched nonlinear crystal. The results show that a tradeoff between a broad bandwidth response and conversion efficiency is not always required, and can be limited to the cases of either a weak pump intensity, or fast changes in phase-mismatch parameter. With an adiabatic design, nearly complete frequency conversion can be achieved, without the necessity of perfect phase matching along the entire propagation. We introduced an important analytical tool, the Landau-Zener conversion efficiency formula, which could estimate the degree of the adiabatic propagation along the SFG process. The robustness of this design for other parameters was also discussed. Among them we explored its robustness to pump intensity, crystal length and acceptance angle variations. We also demonstrated the tunabilty of the broad spectral response via changes of crystal temperature and pump wavelength. This tunability mechanism could have a great impact on the applicability of such devices. While we have demonstrated the method here with a KTP crystal, it can be implemented with any other nonlinear crystal whose second-order nonlinearity can be modulated at high spatial resolution. As an example, in a 20 mm long $LiNbO_3$ having the same chirp parameter, and with the same interacting wavelengths, the spectral bandwidth is slightly narrower, 120 nm instead of 140 nm, but owing to the higher nonlinear coefficient in $LiNbO_3$, lower pump intensity of 310 MW/cm^2 instead of 360 MW/cm^2, would suffice for full conversion.

The adiabatic scheme can be utilized with some care to efficiently upconvert broadband fluorescence signal as well as ultrashort pulses. The present scheme is also highly relevant to spectroscopy of incoherent signals, such as is commonly utilized in astronomy, material science and molecular spectroscopy. Due to the lack of quantum efficient detectors in the mid IR and far IR optical regimes, optically up-converted weak signals into the near IR and visible regimes is often used to facilitate quantum limited detection.

In conclusion, we believe that this scheme is important beyond the obvious practical applications. The complete analogy with two level physics and its geometrical visualization, which is ubiquitous in other physical realms, could bring new physical insights into the process of frequency conversion and will lead to better understanding of other nonlinear optical processes.

This research was supported by Israel Science Foundation (Grants No. 1621/07 and 960/05). H. S. is grateful to the Azrieli Foundation for the award of an Azrieli Fellowship.

#108558 - $15.00 USD Received 11 Mar 2009; revised 14 May 2009; accepted 26 May 2009; published 13 Jul 2009